Polish J. Chem., **75**, 1729–1738 (2001)

Activated Complex in the Decomposition of N_2O over Cu

by S. Polič[1], M. Senegačnik[1], I. Kobal[1*] and M. Zieliński[2]

[1]*J. Stefan Institute, POB 3000, 1000 Ljubljana, Slovenia*
[2]*Jagiellonian University, 30-060 Cracow, Poland*

(Received June 4th, 2001)

Decomposition of N_2O over Cu wire, at initial N_2O pressures 40–60 kPa and temperatures 675–875 K, showed first order kinetics in N_2O with an apparent activation energy of 110 ± 16 kJ mol^{-1}. The ^{15}N and ^{18}O kinetic isotope effects under these experimental conditions were determined and interpreted following the Bigeleisen's formalism. A bent NNO activated complex satisfactorily accounts for the experimental results.

Key words: kinetics, isotope effect, decomposition, activated complex

The decomposition of nitrous oxide has long been of great interest. It was used to characterize the catalytic surfaces and as a model reaction for a number of catalytic systems [1–4]. Its popularity further increased after N_2O was recognized as one of the greenhouse gases, and its catalytic removal from the exhaust of mobile and stationary sources became an urgent environmental problem [5]. Surfaces of metals [6–21], metal oxides [22–42], either pure or supported, alloys [43], perovskites [44], and a variety of zeolites [45–47] have been investigated as catalysts for the reaction. Recently, attention has been focused on the production of N_2 in N_2O decomposition over well-characterized surfaces of transition metals. The high translation energy and direction of desorbing N_2 molecules [48–50] have been explained by a linear N_2O activated complex lying on the surface [48,51–53].

The interaction of N_2O with Cu is interesting from the catalytic point of view [4,29,54–68] and also plays an important role in the production of high-temperature superconductors [69–74]. Adsorption of N_2O on Cu metal is accompanied by an electronic charge transfer from the substrate to N_2O [43,55,59,63,75]. On single crystals, the adsorbed N_2O molecules are oriented normal to the surface, although whether they are attached to the surface by the O or N atom has not yet been clarified [43,61]. The dissociation of N_2O adspecies results into O adatoms and N_2 molecules, which are immediately desorbed [4,29,55,59]. The rate depends strongly on the crystallographic orientation of the surface, the initial reaction probability at room temperature being 0.15 for the (110), 5×10^{-5} for (100) and 10^{-9} for (111) surface [60]. Due to dif-

*The author to whom correspondence should be sent: tel: 00386 1 477 35 80; fax: 00386 1 477 38 11; e-mail: ivan.kobal@ijs.si.

ferences in work function [78,79], the activation energy of dissociation increases, being – 8.5, 13.5, and 43.5 kJ mol^{-1} for these three surfaces in the temperature range of 475–675 K and pressure range of 10–14 μPa [60]. The adsorbed oxygen further reacts to form Cu_2O [4,55,58,76,77]. The overall reaction is first order, or slightly less [55], in N_2O [58,59]. On polycrystalline copper under atmospheric pressure, between 490–580 K, an activation energy of 84 kJ mol^{-1} was obtained [55].

In order to characterize the activated complex in N_2O decomposition over Cu, we have studied nitrogen and oxygen kinetic isotope effects from 675 K to 875 K. The same approach has already been applied successfully to homogeneous N_2O decomposition [80], homogeneous N_2O decomposition catalyzed by bromine [81] and chlorine [82], and N_2O decomposition over MgO [83] and CoO [84].

For the isotopic reactions

$$^{14}N^{14}N^{16}O + 2Cu \xrightarrow{k_o} {}^{14}N^{14}N + Cu_2{}^{16}O$$

$$^{15}N^{14}N^{16}O + 2Cu \xrightarrow{k_1} {}^{15}N^{14}N + Cu_2{}^{16}O$$

$$^{14}N^{15}N^{16}O + 2Cu \xrightarrow{k_2} {}^{14}N^{15}N + Cu_2{}^{16}O$$

$$^{14}N^{14}N^{18}O + 2Cu \xrightarrow{k_3} {}^{14}N^{14}N + Cu_2{}^{18}O$$

^{15}N and ^{18}O kinetic isotope effects (KIE) were defined as KIE(^{15}N) = 100 ($\varepsilon_1 + \varepsilon_2$) and KIE($^{18}O$) = 100 ε_3, where $\varepsilon_i = 1 - k_i/k_o$ and k_i is the rate constant for each reaction. Because N_2O of natural isotopic abundance was used, ε_1 (secondary) and ε_2 (primary) nitrogen effects were not measured separately but the $\varepsilon_1 + \varepsilon_2$ sum was obtained.

EXPERIMENTAL

Apparatus: The same Pyrex glass vacuum system was used as in our previous work and is described elsewhere [81,83]. Its main parts are: 10 dm^3 vessels for storing N_2O and hydrogen, traps for purification and condensation of gases, a Töpler mercury pump to measure pressures and transfer gases, and a 220–250 cm^3 cylindrical quartz reaction vessel (ϕ = 40 mm). The desired reaction temperature was controlled within ±1 K by an electric cylindrical kanthal furnace.

Materials: *Gases*. Pharmaceutical N_2O (Lek Ljubljana, Slovenia) was purified by passage through a trap filled with KOH pellets, followed by several vacuum sublimations between 195 K ($CHCl_3$–CCl_4 1:1 mixture in liquid nitrogen) and 77 K (liquid nitrogen). High-purity grade hydrogen (GTW, Munich, Germany) was used without further purification.

Catalyst. Reagent grade (99.9%) electrolytic copper wire of 0.21 mm diameter (SAFI, Milano, Italy) was used. In order to facilitate handling, the wire was shaped into *ca*. 40 cm long spirals with a diameter of *ca*. 0.4 cm. Spirals were degreased for 16 hours by benzene in a reflux apparatus and then introduced into the reaction vessel. After 2–3 hour outgassing at a background pressure of 10 mPa, spirals were oxidized by 1.5 mmole of N_2O and regenerated with excess hydrogen, this treatment being repeated several times. The geometric specific surface area was 0.21 m^2 g^{-1}.

Procedures: Detailed descriptions of all procedures are given elsewhere [81,83].

Kinetic runs: Prior to every experiment, the Cu wire was regenerated by hydrogen as described above. The following masses of wire were used: 80 g at temperature 675 K, 8 g at 775 K and 3.7 g at 875 K. N_2O was introduced to a pressure of 40–60 kPa at room temperature. Because there is no volume change, the pressure of residual N_2O during the reaction was obtained by measuring the pressure of N_2 after N_2O had been condensed.

KIE determinations: Nitrogen and oxygen kinetic isotope effects were determined at 675, 775 and 875 K. Prior to each run, the catalyst was regenerated by hydrogen. N_2O was introduced to a pressure 40–60 kPa at room temperature.

After 70–90% of N_2O decomposition, the reaction was stopped by removing the furnace and cooling the vessel to room temperature. By means of the Töpler mercury pump the reaction gas mixture was pumped back and forth through a trap cooled with liquid nitrogen in order to freeze out residual N_2O. The N_2O was purified by repeated sublimation between 195 and 77 K (as described above). The extent of reaction, f, was obtained from the initial, $P^o_{N_2O}$, and final N_2O pressures, $P^f_{N_2O}$, measured at room temperature using the expression $f = 1 - (P^f_{N_2O}/P^o_{N_2O})$. In order to remove any traces of CO_2, N_2O was kept overnight in a vessel with a freshly prepared KOH mirror, then sealed into a glass ampoule, and stored for isotopic analysis. The isotopic mass ratios $R_1 = [^{15}N^{14}N^{16}O]/[^{14}N^{14}N^{16}O]$, $R_2 = [^{14}N^{15}N^{16}O]/[^{14}N^{14}N^{16}O]$, and $R_3 = [^{14}N^{14}N^{18}O]/[^{14}N^{14}N^{16}O]$ in the initial N_2O (denoted below by ^{o}) and in the residual N_2O (denoted by ^{f}) were measured by a Nier-M^{c}Kinney type double collector mass spectrometer [81,83]. Both $^{15}N^{14}N^{16}O$ and $^{14}N^{15}N^{16}O$ species contribute to the mass of 45, so the sum of the nitrogen effects was determined, but not the individual effects. Kinetic isotope effects were calculated by applying the formulae [85,86]

$$KIE(^{15}N) = 100(\varepsilon_1 + \varepsilon_2) = 200\,\frac{S(^{45}_{44}) - 1}{\log(1 - f)}; \qquad KIE(^{18}O) = 100\varepsilon_3 = -100\frac{\log S(^{46}_{44})}{\log(1 - f)}$$

where $S(^{45}_{44}) = (R_1^f + R_2^f)/(R_1^o + R_2^o)$ and $S(^{46}_{44}) = R_3^f/R_3^o$.

RESULTS AND DISCUSSION

Kinetics: Several typical kinetic runs are presented in Fig. 1. The straight lines show that the data fit first order kinetics expressed as

$$\frac{dP_{N_2O}}{dt} = -kP_{N_2O}\frac{A}{V}$$

where k is the rate constant of the overall reaction ($\mu m\ s^{-1}$), A is the catalyst surface area (m^2) and V is the volume (m^3) of the reaction vessel. At each temperature 5 to 8 experiments were carried out and the average values of the rate constants are collected in Table 1. The desired reproducibility was achieved after 3–4 reduction/oxidation cycles of the catalyst before the kinetic run. The Arrhenius plot gives an apparent activation energy of 110 ± 16 kJ mol^{-1}, which is about 20% lower than the previously obtained value [55].

Kinetic isotope effects: Temperatures, extents of reaction, nitrogen and oxygen kinetic isotope effects are given in Table 2. Their temperature dependence is expressed by: $KIE(^{15}N) = (0.377 \pm 0.216) + (1698 \pm 164)/T$ and $KIE(^{18}O) = (1.95 \pm 0.06) + (1678 \pm 44)/T$.

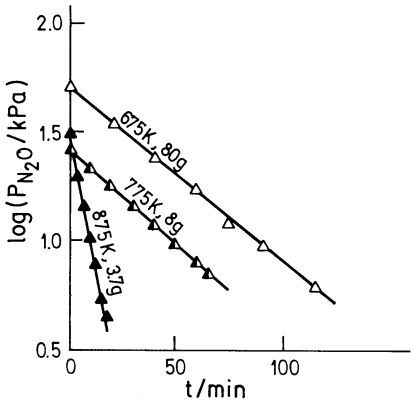

Figure 1. Kinetics of N_2O decomposition on Cu wire. Reaction temperature and mass of the wire used are indicated on each plot.

Table 1. Rate constants in N_2O decomposition on Cu at different temperatures.

T/K	675	775	875
k/μm s^{-1}	37 ± 5	210 ± 30	3600 ±400

Table 2. Temperature, extent of reaction, and experimental KIE(^{15}N) and KIE(^{18}O) values for N_2O decomposition on Cu.

T/K	f	KIE(^{15}N)	KIE(^{18}O)
675	0.874	2.9	4.4
	0.832	2.9	4.5
	0.851	2.9	4.5
	0.881	2.7	4.4
	0.899	2.8	4.3
	0.865	3.0	4.4
	0.858	3.0	4.5
	0.886	2.8	4.5
675	average	2.88 ± 0.10	4.44 ± 0.07
775	0.860	2.5	4.1
	0.834	2.7	4.0
	0.843	2.7	4.2
	0.724	2.5	4.1
	0.774	2.5	4.2
	0.818	2.7	4.2
775	average	2.6 ± 0.11	4.13 ± 0.08
875	0.869	2.2	3.9
	0.913	2.2	3.9
	0.856	2.5	3.8
	0.855	2.3	3.9
	0.800	2.2	3.9
	0.812	2.4	3.8
875	average	2.30 ± 0.13	3.87 ± 0.05

As in our previous work, the results are interpreted using the Bigeleisen's formula to calculate the harmonic rate ratios [83–86]

$$\frac{k_0}{k_1} = \frac{\nu_{Lo}^{\neq}}{\nu_{Li}^{\neq}} \prod_{j=1}^{3n-6} \frac{u_{ij}\sinh(u_{oj}/2)}{u_{oj}\sinh(u_{ij}/2)} \prod_{j=1}^{3n^{\neq}-7} \frac{u_{oj}^{\neq}\sinh(u_{ij}^{\neq}/2)}{u_{ij}^{\neq}\sinh(u_{oj}^{\neq}/2)}$$

in which ≠ denotes the transition state. The first product includes all the isotopic frequencies of the N_2O reactant molecule and the second one the real frequencies of the transition state. ν_L is the frequency of the normal mode belonging to the reaction coordinate, and $u = hc\omega/(k_BT)$, where ω – wave number in cm^{-1}, h – Planck's constant, k_B – Boltzmann's constant, c – speed of light, T – temperature.

The isotopic frequencies of the transition state were obtained by solving Wilson's FG matrix equation [83–88]

$$\mathbf{GFL} = \mathbf{L}\Lambda$$

in which **G** is the Wilson matrix of kinetic energy, **F** is the force-constant matrix, **L** is the eigenvector matrix and Λ is a diagonal matrix of eigenvalues $\lambda_{ii} = 4\pi^2\nu_i^2$ with ν_i being the frequency of the *i*th normal vibration.

The gaseous N_2O molecule is considered to be in thermodynamic equilibrium with the transition state. The interaction of the transition state with the surface was not taken into account [86]. Isotopic normal frequencies for the reactant N_2O molecule were taken from the literature [89]. For the activated complex a linear NNO was suggested, with its asymmetric normal mode of vibration as the reaction coordinate [57]. In order to be more general, in our calculations we took into consideration angles from 90° to 180° in steps of 10°. The force constant of the N–N bond (D), F_D, ranged from 1400 to 2600 Nm^{-1}, the force constant of the N–O bond (d), F_d, ranged from 100 to 1000 Nm^{-1} (both in steps of 100 Nm^{-1}), while the bending force constant for the N–N–O interbond angle α, F_α, was fixed at 40, 70 or 100 Nm^{-1}. As required for the zero frequency of the reaction coordinate [83], the interaction force constant of the N–N and N–O bonds was conditioned by $F_{Dd} = +(F_D F_d)^{1/2}$. Bond lengths (in pm) were calculated from force constants (in Nm^{-1}) using the empirical relationships [90,91]: $D = 100\,(3730/F_D)^{1/5.71}$ and $d = 100\,(3440/F_d)^{1/5.97}$. For all the combinations of parameter values stated above, theoretical nitrogen and oxygen kinetic isotope effects for the three temperatures were calculated and compared with the experimental data. As an example, the ranges of values of the (F_D, F_d) pairs giving agreement with experiment within $\pm 1\sigma$ (standard deviation) are drawn separately for ^{15}N (Fig. 2) and ^{18}O (Fig. 3) effects. Only the dashed region is interesting for us: here, the regions for the three temperatures overlap, showing that the same (F_D, F_d) combination is successful, providing agreement with experiment over the whole temperature range studied. If Fig. 2 and Fig. 3 are combined, Fig. 4 is obtained, showing by its dashed region those (F_D, F_d) values successful both for ^{15}N and ^{18}O effects. Results of all calculations are summarized in Fig. 5. It is evident that angles below 100° and above 130°

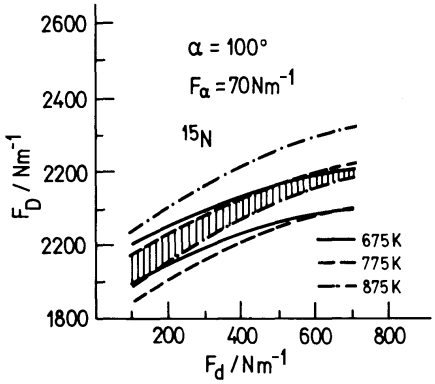

Figure 2. Ranges of (F_D, F_d) values for the NNO-bent activated complex, which for $\alpha = 100°$ and $F_\alpha = 70$ Nm^{-1}, provide agreement with experimental ^{15}N kinetic isotope effects at the three temperatures.

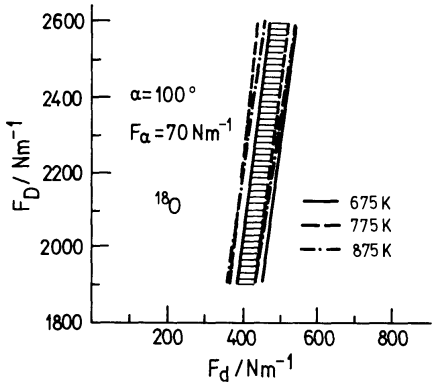

Figure 3. Ranges of (F_D, F_d) values for the NNO-bent activated complex, which for $\alpha = 100°$ and $F_\alpha = 70$ Nm^{-1}, provide agreement with experimental ^{18}O kinetic isotope effects at the three temperatures.

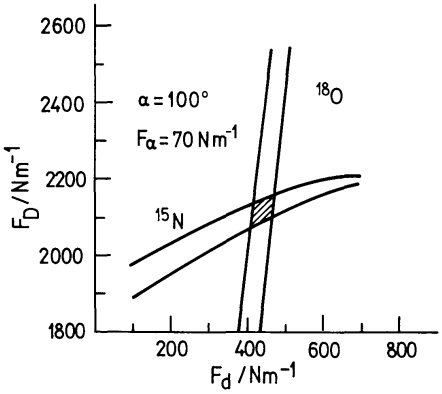

Figure 4. (F_D, F_d) values for the NNO-bent activated complex, which for $\alpha = 100°$ and $F_\alpha = 70$ Nm^{-1}, provide agreement with experimental ^{15}N and ^{18}O kinetic isotope effects, shown by the dashed region.

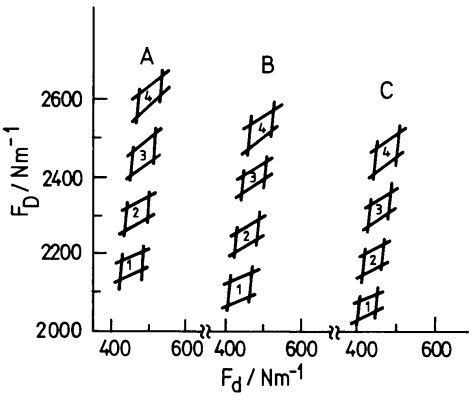

Figure 5. Regions of (F_D, F_d) values for the NNO-bent activated complex, which for selected α and F_α, provide agreement with experimental ^{15}N and ^{18}O kinetic isotope effects. F_α/ Nm^{-1}: A = 40, B = 70, and C = 100. α: 1 = 100°, 2 = 110°, 3 = 120°, 4 = 130°.

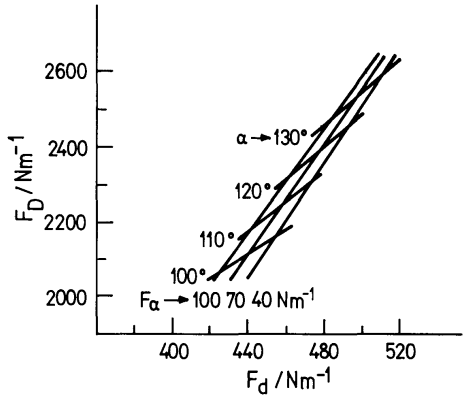

Figure 6. Regions of F_D, F_d, F_α, and α values of the NNO-bent activated complex, which provide agreement with experimental ^{15}N and ^{18}O kinetic isotope effects.

were not successful. For a selected F_α, only a slight increase in F_d is seen with increasing α, while the increase in F_D is substantial. The opposite effect is seen for F_α: for a selected α, both F_D and F_d decrease with increasing F_d, that for F_D being more pronounced. If we take centres of parallelograms from Fig. 5 and replot them in Fig. 6, we finally see the entire region of parameter values, which provide agreement with experiment.

Our calculations reveal a bent NNO activated complex. Although this geometry cannot be proven experimentally, it is anticipated from theoretical considerations, especially if electronic charge transfer or excitation is taken into account [92–95]. F_D values of the activated complex would be expected to be higher than the experimental values of 1819–1859 Nm^{-1} for the N–N bond in N_2O [96], but comparable to the values obtained by quantum chemical calculations, reaching even 2650 Nm^{-1} [96–98]. If we further assume that F_D in the activated complex is expected to be lower than about 2300 Nm^{-1} (the experimental value in N_2 [99]) then only angles between 100° and 110° from Fig. 6 are acceptable. Because, on the other hand, the calculated force con-

stants for the N–N bond in N_2 are as high as 2500 Nm^{-1} [99], we may extent the acceptable region up to 130° (see Fig. 6). This α value, which also has a theoretical background [92], can also be used if higher F_α values and concomitantly lower F_D values are taken. Nevertheless, F_α values much higher than 100 Nm^{-1} are not reasonable [96–98]. The F_d value in the activated complex should lie between zero and about 1200 Nm^{-1}, the value in gaseous N_2O [96–98]. Values of 420–520 Nm^{-1} in Fig. 6 fit this requirement.

As an example of the success of our proposed geometry for the activated complex, lines of calculated kinetic isotope effects, obtained by a selected combination of parameter values from Fig. 6, are drawn through the experimental points in Fig. 7 and satisfactory agreement is evident.

Because the simple bent NNO activated complex satisfactorily reproduces the magnitude and temperature dependence of both ^{15}N and ^{18}O kinetic isotope effects, we have not extended our study to more complicated structures [83,100–102].

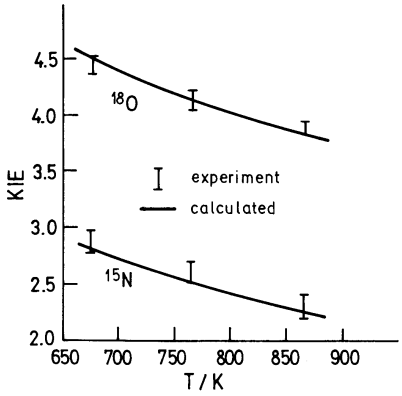

Figure 7. Comparison of calculated ^{15}N and ^{18}O kinetic isotope effects for the NNO-bent activated complex with experimental values, $\alpha = 100°$, $F_D = 2100$ Nm^{-1}, $F_d = 440$ Nm^{-1}, $F_\alpha = 70$ Nm^{-1}.

CONCLUSIONS

The decomposition of N_2O on Cu over the temperature range from 675 to 875 K and at initial N_2O pressures between 40 and 60 kPa was found to be first order in N_2O with an activation energy of 110 ± 16 kJ mol^{-1}. The interpretation of experimental nitrogen and oxygen kinetic isotope effects led to a bent NNO activated complex, values of parameters being in the following ranges: $F_D = 2100$–2500 Nm^{-1}, $F_d = 420$–520 Nm^{-1}, $F_\alpha = 40$–100 Nm^{-1} and $\alpha = 100$–$130°$. A linear NNO activated complex does not lead to an agreement with experiment. More complicated, four atom activated complexes have not been checked.

Acknowledgments

This study was funded by the Ministry of Education, Science and Sport of Slovenia. The authors thank to Ms Lilijana Per for her figures.

REFERENCES

1. Johnston H.S.J., *Chem. Phys*., **19**, 663 (1951).
2. Werner G.M. and Marcus R.A.J., *Chem. Phys*., **37**, 1835 (1962).
3. Ertl G., *Surf. Sci*., **6**, 208 (1967).
4. Kapteijn F., Rodriguez-Mirasol J. and Moulijn J.A., *Appl. Catal*. *B*, **9**, 25 (1996).
5. Pârvulescu V., Grange P. and Delmon B., *Catal. Today*, **46**, 233 (1998).
6. Redmond J.P., *J. Catal*., **7**, 297 (1967).
7. Cimino A. and Schiavello M., *J. Catal*., **20**, 202 (1971).
8. Weinberg W.H., *J. Catal*., **28**, 459 (1973).
9. Shi S.–K., Lee H.–I. and White J.M., *Surf. Sci*., **102**, 56 (1981).
10. Wicke B.G., *J. Chem. Phys*., **78**, 6036 (1983).
11. Raiche G.A. and Belbruno J.J., *Chem. Phys. Lett*., **134**, 341 (1987).
12. Kiss J., Jo S.J. and White J.M., *J. Phys. Chem*., **95**, 8054 (1991).
13. Blazej M. and March N.H., *J. Molec. Struct. (Theochem)*, **312**, 127 (1994).
14. Stirling A., *J. Phys. Chem. A*, **102**, 6565 (1998).
15. Zhu Z.H., Wang S., Lu G.Q. and Zhang D.-K., *Catal. Today*, **53**, 669 (1999).
16. Zhu Z.H. and Lu G.Q., *J. Catal*., **187**, 262 (1999).
17. Vetter R., Naulin C. and Costes M., *Phys. Chem. Chem. Phys*., **2**, 643 (2000).
18. Pinna F., Scarpa M., Strukul G., Guglielminotti E., Boccuzzi F. and Manzoli M., *J. Catal*., **192**, 158 (2000).
19. Centi G., Dall'Olio L. and Perathoner S., *J. Catal*., **192**, 224 (2000).
20. Centi G., Dall'Olio L. and Perathoner S., *J. Catal*., **194**, 130 (2000).
21. Sano T., Negishi N., Mas D. and Takeuchi K., *J. Catal*., **194**, 71 (2000).
22. Hauffe K. and Schlosser E.-G., *Z. Elektrochem*., **61**, 506 (1957).
23. Dewing J. and Cvetanović R.J., *Can. J. Chem*., **36**, 678 (1958).
24. von Schulz I., Scheve J. and Rienäcker G.Z., *Z. Anorg. Allg. Chem*., **352**, 231 (1967).
25. Lisachenko A.A. and Vilesov F.I., *Kinet. Katal*., **9**, 935 (1968).
26. Guilleux M.-F. and Imelik B., *Bull. Soc. Chim. Fr*., 1340 (1970).
27. von Schulz W.D. and Scheve J., *Z. Anorgan. Allg. Chem*., **366**, 231 (1969).
28. Winter E.R.S., *J. Catal*., **15**, 144 (1969).
29. Winter E.R. S., *J. Catal*., **19**, 32 (1970).
30. Tanaka K. and Blyholder G., *J. Phys. Chem*., **75**, 1037 (1971).
31. Cunningham J., Kelly J.J. and Penny A.L., *J. Phys. Chem*., **75**, 617 (1971).
32. Zecchina A., Cerruti and Borello L.E., *J. Catal*., **25**, 55 (1972).
33. Kazusaka A. and Lunsford J.H., *J. Catal*., **45**, 25 (1976).
34. Dupont-Pavlovsky N. and Caralp F., *J. Catal*., **46**, 426 (1977).
35. Morterra C., Boccuzzi F., Coluccia S. and Ghiotti G., *J. Catal*., **65**, 231 (1980).
36. Busca G. and Lorenzelli V., *J. Catal*., **72**, 303 (1981).
37. Nakamura M., Mitsuhashi H. and Takezawa N., *J. Catal*., **138**, 686 (1992).
38. Miller T.M. and Grassian V.H., *Colloid. Surf*., **105**, 113 (1995).
39. Kantorovich L.N. and Gillan M.J., *Surf. Sci*., **376**, 169 (1997).
40. Snis A. and Miettinen H., *J. Phys. Chem. B*, **102**, 2555 (1998).
41. Overbury S.H., Mullins D.R., Huntley D.R. and Kundakovic L., *J. Catal*., **186**, 296 (1999).
42. Lu X., Xu X., Wang N. and Zhang Q., *J. Phys. Chem. B*, **103**, 3373 (1999).
43. Pashusky A. and Folman M., *Surf. Sci*., **244**, 197 (1991).
44. Raj S.L. and Srinivasan V., *J. Catal*., **65**, 121 (1980).
45. Petunchi J.O. and Hall W.K., *J. Catal*., **78**, 327 (1982).
46. Leglise J., Petunchi J.O. and Hall W.K., *J. Catal*., **86**, 392 (1984).
47. Kapteijn F., Marbán G., Rodriguez-Mirasol J. and Moulijn J.A., *J. Catal*., **167**, 256 (1997).
48. Ohno Y., Kimura K., Bi M. and Matsushima T., *J. Chem. Phys*., **110**, 8221 (1999).
49. Kato H., Lee J., Sawabe K. and Matsumoto Y., *Surf. Sci*., **445**, 209 (2000).
50. Haq S. and Hodgson A., *Surf. Sci*., **463**, 1 (2000).
51. Ohno Y., Kobal I., Kimura K., Horino H. and Matsushima T., *Catalysts & Catal*., **41**, 421 (1999).
52. Kobal I., Kimura K., Ohno Y. and Matsushima T., *Surf. Sci*., **445**, 472 (2000).
53. Kobal I. and Matsushima T., *Trends in Chem. Phys*., **7**, 169 (1999).

54. Dell R.M., Stone F.S. and Tiley P.F., *Trans. Farad. Soc*., **49**, 195 (1953).
55. Dell R.M., Stone F.S. and Tiley P.F., *Trans. Farad.* **49**, 201 (1953).
56. Osinaga T.J., Linsen B.G. and van Beek W.P., *J. Catal*., **7**, 277 (1967).
57. Bass H.E. and Fanchi J.R., *J. Chem. Phys*., **64**, 4417 (1976).
58. Habraken F.H.P.M., Kieffer E.P. and Bootsma G.A., *Surf. Sci*., **83**, 45 (1979).
59. Habraken F.H.P.M. and Bootsma G.A., *Surf. Sci*., **87**, 45 (1979).
60. Habraken F.H.P.M., Mesters C.M.A.M. and Bootsma G.A., *Surf. Sci*., **97**, 264 (1980).
61. Spitzer A. and Lüth H., *Phys. Rev. B*, **30**, 3098 (1984).
62. Döbler U. and Baberschke K., *Surf. Sci*., **152**/**153**, 569 (1985).
63. Arlow J.S. and Woodruff D.P., *Surf. Sci*., **157**, 327 (1985).
64. Turek T., *J. Catal*., **174**, 98 (1998).
65. Morterra C., Giamello E., Giamello G., Centi G. and Perathoner S., *J. Catal*., **179**, 111 (1998).
66. Ciambelli P., di Benedetto A., Garufi E., Pirone R. and Russo G., *J. Catal*., **175**, 161 (1998).
67. Matsuoka M., Ju W.–S., Takahashi K., Yamashita H. and Anpo M., *J. Phys. Chem. B*, **104**, 4911 (2000).
68. Hårsta A. and Carlsson J.–O., *J. Crystal Grouth*, **114**, 507 (1991).
69. Schwab P., Kochemasov A., Kullmer R. and Bäuerle D., *Appl. Phys. A*, **54**, 166 (1992).
70. Katayama S., Mizushima Y. and Sekine M., *J. Appl. Phys.*, **71**, 1534 (1992).
71. Otis C.E., Gupta A. and Braren B., *Appl. Phys. Lett.*, **62**, 1534 (1993).
72. Willmott P.R., Timm R., Felder P. and Huber J.R., *J. Appl. Phys.*, **76**, 2657 (1994).
73. Ottosson M., Lu J. and Carlsson J.–O., *J. Crystal Grouth*, **151**, 305 (1995).
74. Johnson C.N.L., Helmersson U., Madsen L.D., Rudner S. and Wernlund L.–D., *J. Appl. Phys.*, **77**, 6388 (1995).
75. Sears J.T., *J. Phys. Chem.*, **73**, 1143 (1969).
76. Benndorf C., Egert B., Keller G. and Thieme F., *Surf. Sci*., **74**, 216 (1978).
77. Döbler U. and Baberschke K., *Phys. Rev. Lett.,* **52**, 1437 (1984).
78. Delchar T.A., *Surf. Sci*., **27**, 11 (1971).
79. Gartland P.O., Berge S. and Slagsvold B.J., *Phys. Rev. Lett*., **28**, 738 (1972).
80. Zieliński M., *C-13, C-14 and O-18 Kinetic Isotope Effects in Some Chemical Reactions*, Habilitation Thesis, University of Warsaw, Poland, (1966).
81. Lesar A. and Senegačnik M., *J. Chem. Phys*., **99**, 187 (1993).
82. Lesar A., Hodošček M. and Senegačnik M., *J. Chem. Phys*., **105**, 917 (1996).
83. Zemva P., Lesar A., Senegačnik M. and Kobal I., *Phys. Chem. Chem. Phys*., **2**, 3319 (2000).
84. Zemva P., Senegačnik M. and Kobal I., in: L. Petrov, Ch. Bonev and G. Kadinov (Eds), Proc. 9th Int. Symp., *Heterogeneous Catalysis*, Varna, Bulgaria, p. 139 (2000).
85. Bigeleisen J. and Wolfsberg M., *Adv. Chem. Phys*., **1**, 15 (1958).
86. van Hook W. A., in: C.J. Collins and N.S. Bowman (Eds), *Isotope Effects in Chemical Reactions*, Van Nostrand-Reinhold, NY, p. 1 (1970).
87. Guns P., *Vibrating Molecule*, Chapman & Hall, London, (1971).
88. Wilson E.B., Decius J.C. and Cross P.C., *Molecular Vibrations*, McGraw-Hill, NY, (1965).
89. Bigeleisen J. and Friedman L., *J. Chem. Phys*., **18**, 1656 (1950).
90. Thomas T.H., Ladd J.A., Jones I.P. and Orville-Thomas W.J., *J. Mol. Struct*., **3**, 49 (1969).
91. Ladd J.A. and Orville-Thomas W.J., *Spectrochim. Acta*, **22**, 919 (1969).
92. Hopper D.G., *J. Chem. Phys*., **80**, 4290 (1984).
93. Masson D.P., Lanzendorf E.J. and Kummel A.C., *J. Chem. Phys*., **102**, 9096 (1995).
94. Harcourt R.D. and Hall N., *Theochem*, **342**, 59 (1995).
95. Wang F. and Harcourt R.D., *J. Phys. Chem. A*, **104**, 1304 (2000).
96. Martin J.L.M., Taylor P.R. and Lee T.J., *Chem. Phys. Lett*., **205**, 535 (1993).
97. Allen W.D., Yamaguchi Y., Császár A.G., Clabo D.A. Jr., Remington R.B. and Schaeffer III H.F., *Chem. Phys.*, **145**, 427 (1990).
98. Yan G., Xian H. and Xie D., *Chem. Phys. Lett*., **271**, 157 (1997).
99. Császár A.G., *J. Phys. Chem. A*, **98**, 8823 (1994).
100. Zemva P., Lesar A., Senegačnik M. and Kobal I. *Langmuir*, **17**, 1543 (2001).
101. Zemva P., Lesar A., Senegačnik M. and Kobal I., *Chem. Phys*., **264**, 413 (2001).
102. Zemva P., Lesar A., Senegačnik M. and Kobal I., *Phys. Chem.*, (2001) in press.